

ChemSusChem

Supporting Information

Molecular Functionalization of NiO Nanocatalyst for Enhanced Water Oxidation by Electronic Structure Engineering

Lizhou Fan, Biaobiao Zhang, Zhen Qiu, N. V. R. Aditya Dharanipragada, Brian J. J. Timmer, Fuguo Zhang, Xia Sheng, Tianqi Liu, Qijun Meng, A. Ken Inge, Tomas Edvinsson, and Licheng Sun*© 2020 The Authors. Published by Wiley-VCH GmbH. This is an open access article under the terms of the Creative Commons Attribution Non-Commercial License, which permits use, distribution and reproduction in any medium, provided the original work is properly cited and is not used for commercial purposes. This publication is part of a Special Collection highlighting “The Latest Research from our Board Members”. Please visit the Special Collection at <https://bit.ly/cscBoardMembers>.

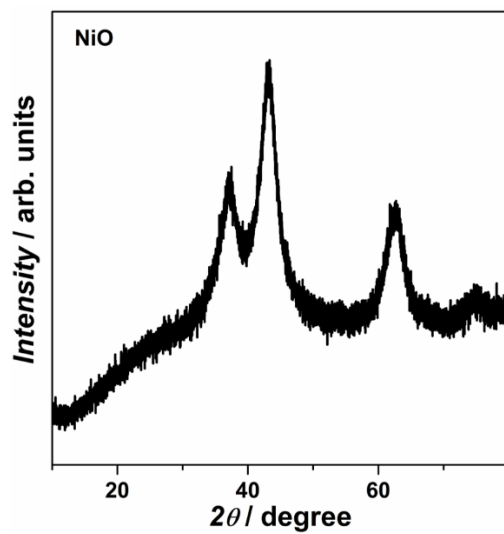


Figure S1 XRD pattern of as-prepared ultrasmall NiO nanoparticles.

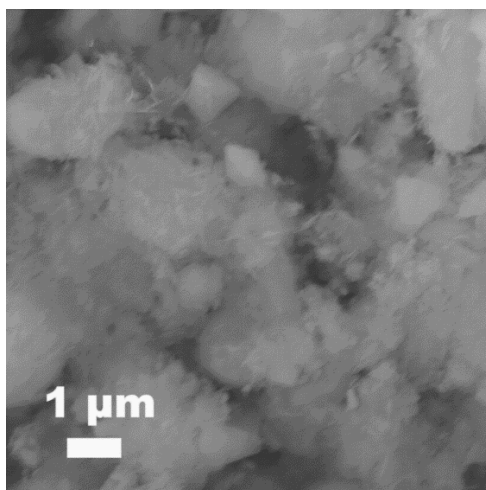


Figure S2 SEM image of as-prepared ultrasmall NiO nanoparticles.

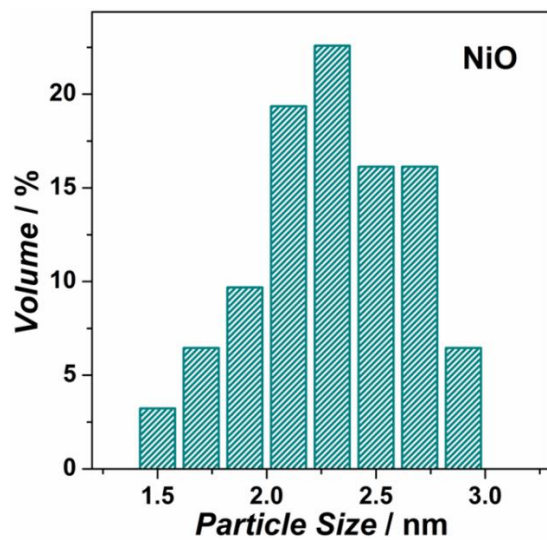


Figure S3 Particle size distribution of ultrasmall NiO nanoparticles.

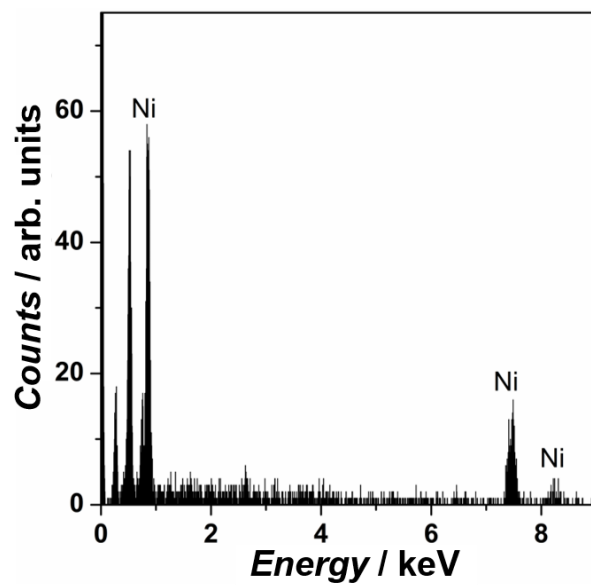


Figure S4 EDS spectrum of as-prepared ultrasmall NiO nanoparticles.

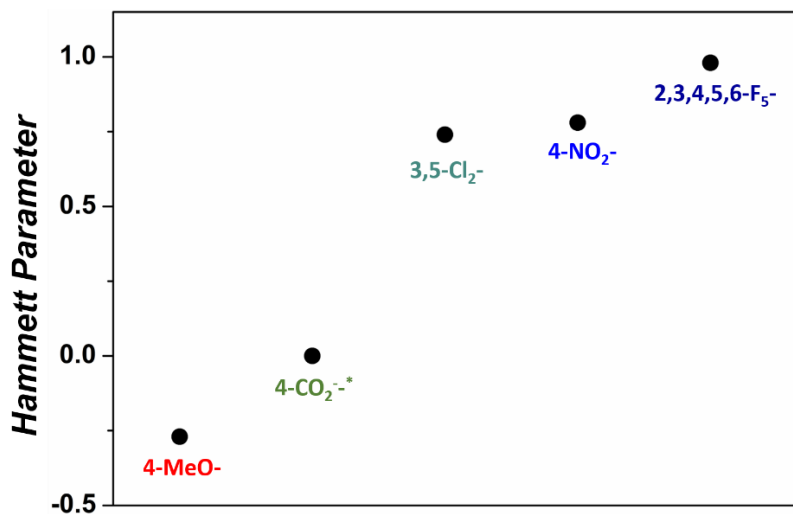


Figure S5 The Hammett parameter of substitutions on all modified molecules. * The -CO₂H group is deprotonated under alkaline OER conditions (-CO₂⁻), behaving as electron-neutral property.

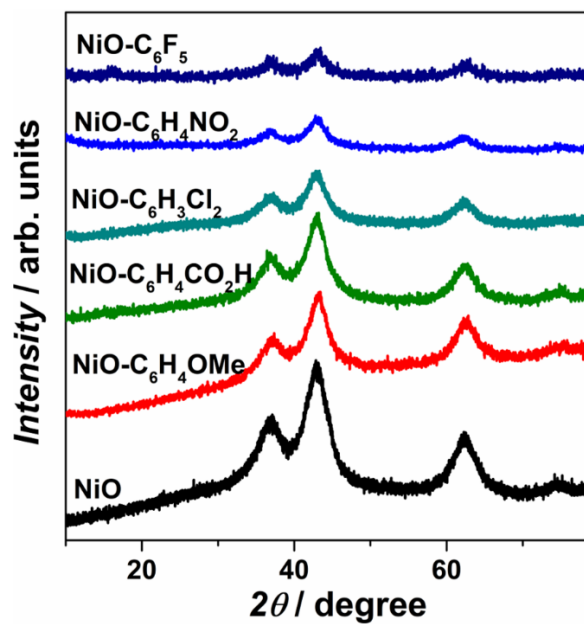


Figure S6 XRD patterns of pristine and molecularly modified ultrasmall NiO nanoparticles.

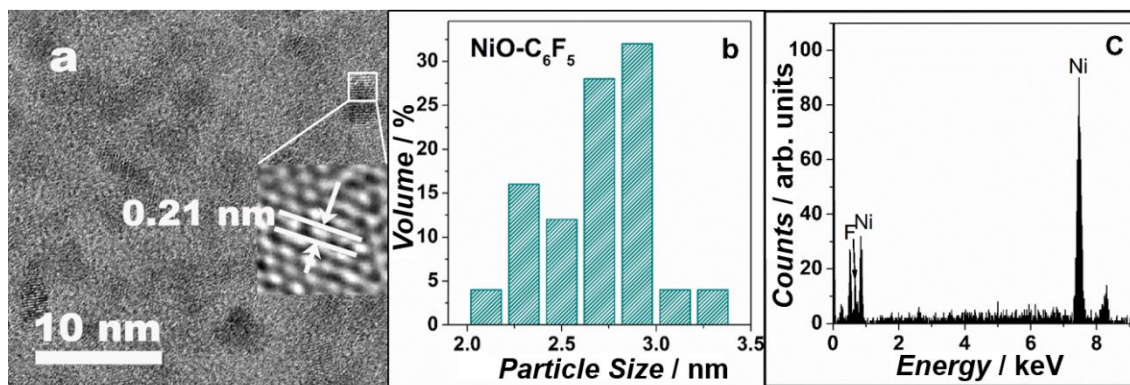


Figure S7 a) TEM pattern, b) Particle size distribution and c) EDS spectrum of NiO-C₆F₅ sample.

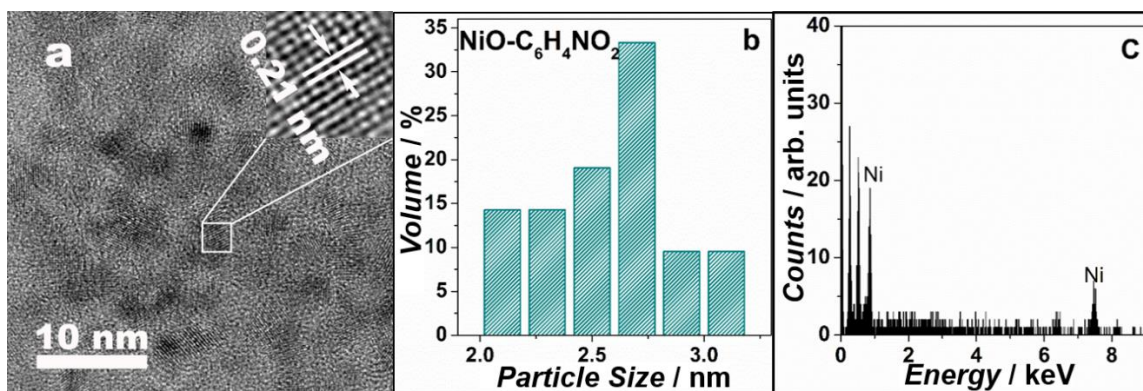


Figure S8 a) TEM pattern, b) Particle size distribution and c) EDS spectrum of NiO-C₆H₄NO₂ sample.

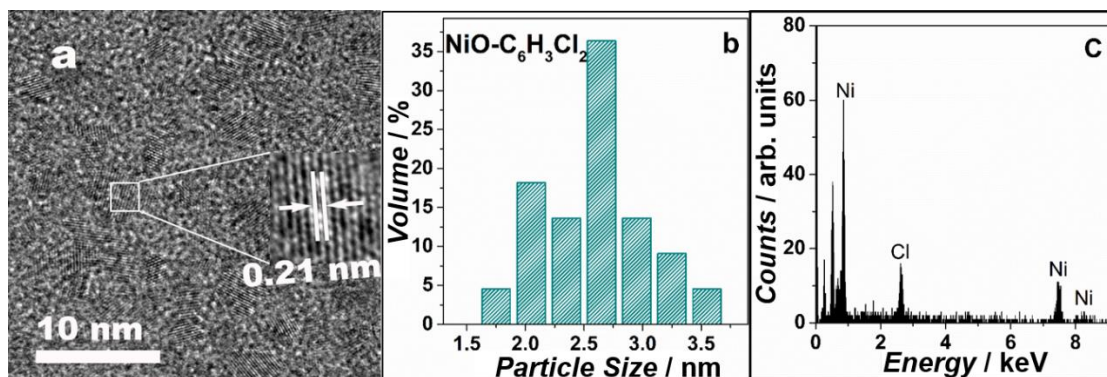


Figure S9 a) TEM pattern, b) Particle size distribution and c) EDS spectrum of NiO-C₆H₃Cl₂ sample.

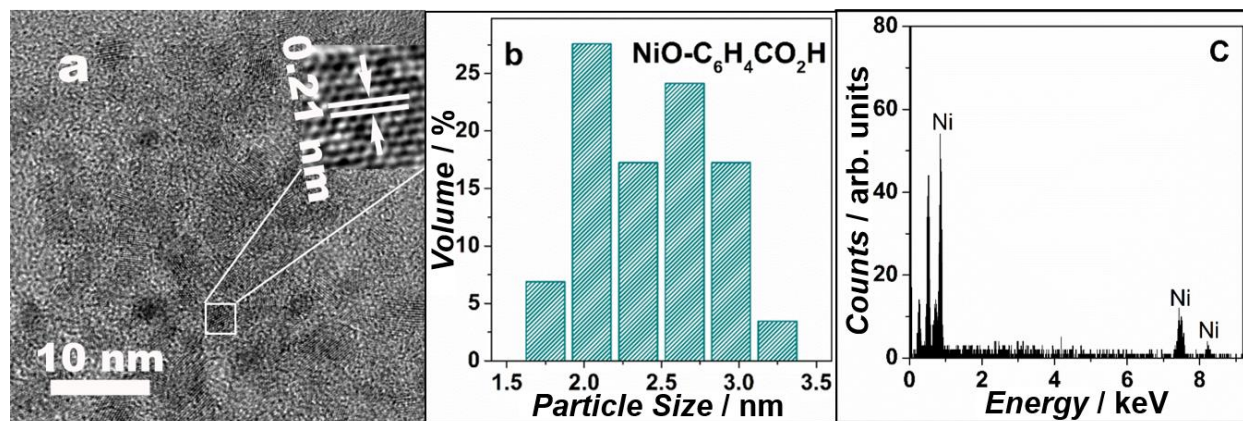


Figure S10 a) TEM pattern, b) Particle size distribution and c) EDS spectrum of NiO-C₆H₄CO₂H sample.

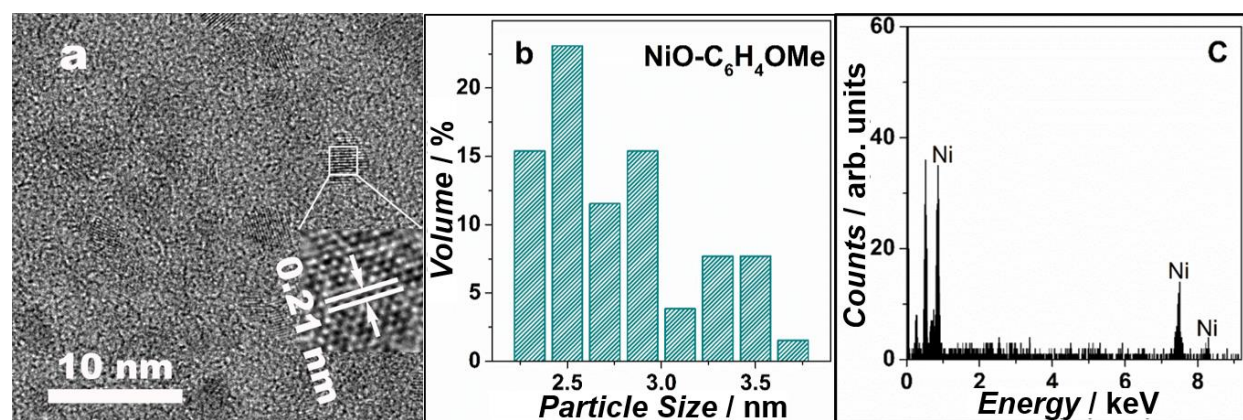


Figure S11 a) TEM pattern, b) Particle size distribution and c) EDS spectrum of NiO-C₆H₄OMe sample.

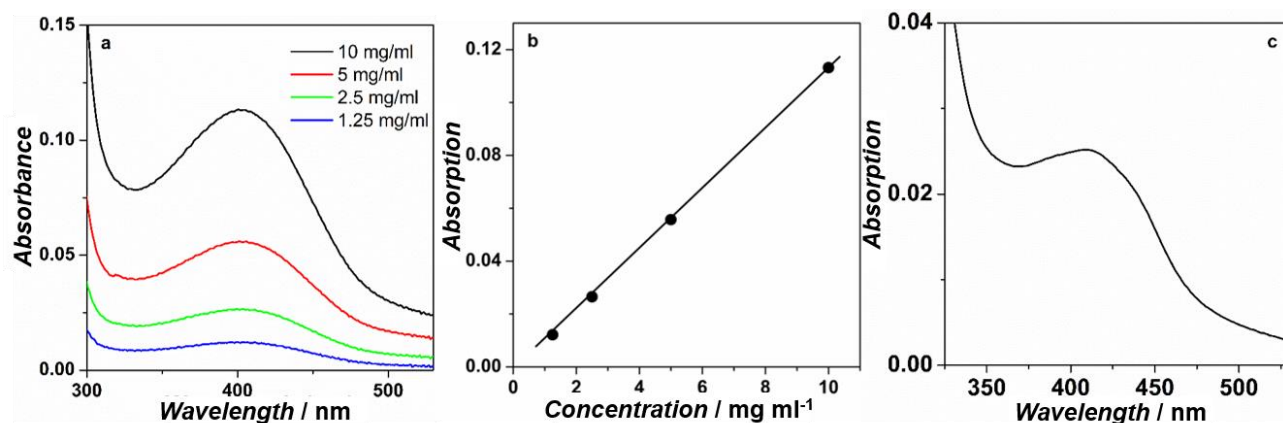


Figure S12 a) UV-Vis spectrum of pentafluorophenyldiazonium tetrafluoroborate solution at different concentrations. b) Plot of absorption at 405 nm versus concentration. c) UV-vis spectrum of pentafluorophenyldiazonium tetrafluoroborate solution after molecular modification of NiO nanoparticles. The concentration of diazonium salt remaining in solution is estimated to be 2.18 mg/ml and the loaded molecule amount is estimated to be 2.11 nm⁻².

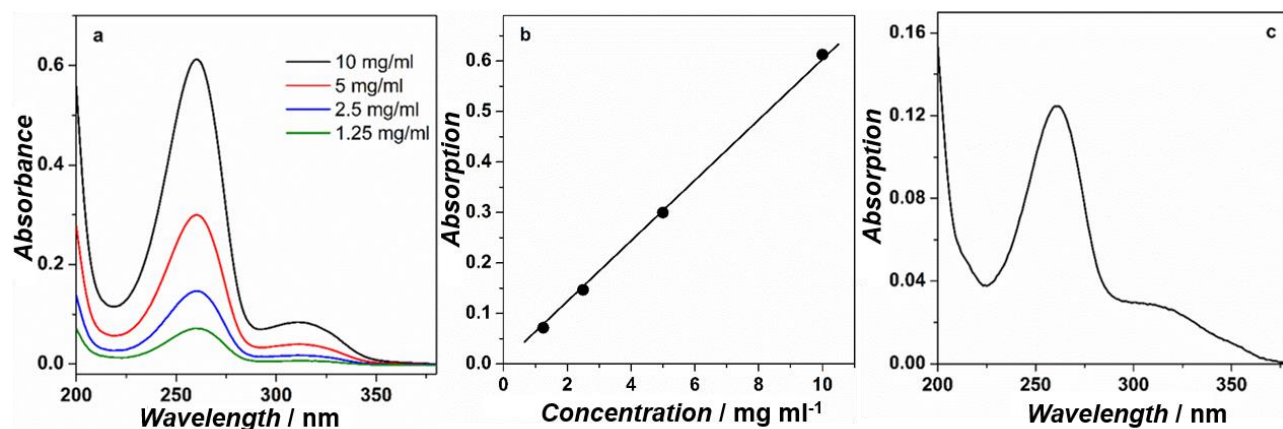


Figure S13 a) UV-Vis spectrum of 4-nitrobenzenediazonium tetrafluoroborate solution at different concentrations. b) Plot of absorption at 260 nm versus concentration. c) UV-Vis spectrum of 4-nitrobenzenediazonium tetrafluoroborate solution after molecular modification of NiO nanoparticles. The concentration of diazonium salt remaining in solution is estimated to be 2.06 mg/ml and the loaded molecule amount is estimated to be 2.55 nm⁻².

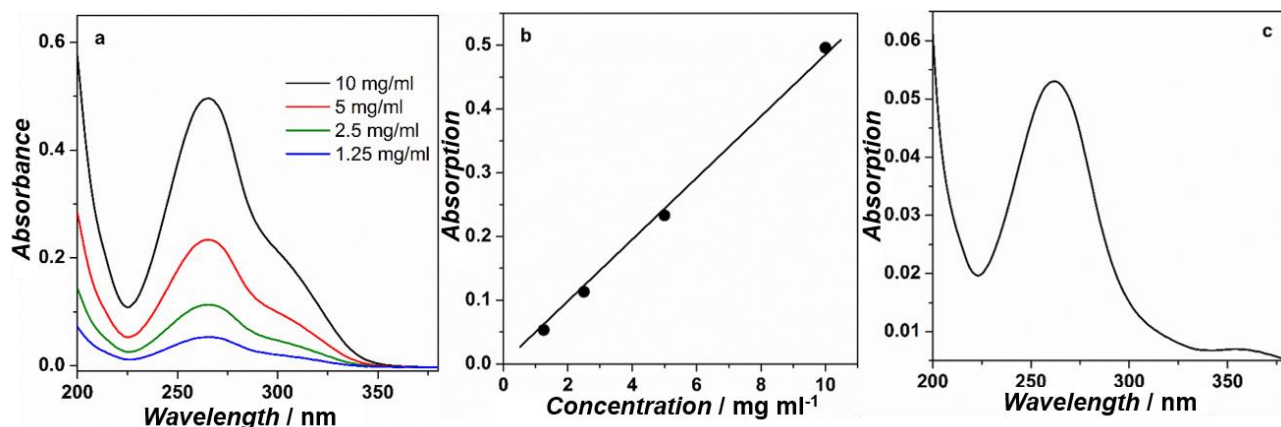


Figure S14 a) UV-Vis spectrum of 4-carboxylbenzenediazonium tetrafluoroborate solution at different concentrations. b) Plot of absorption at 260 nm versus concentration. c) UV-Vis spectrum of 4-carboxylbenzenediazonium tetrafluoroborate solution after molecular modification of NiO nanoparticles. The concentration of diazonium salt remaining in solution is estimated to be 1.18 mg/ml and the loaded molecule amount is estimated to be 3.31 nm⁻².

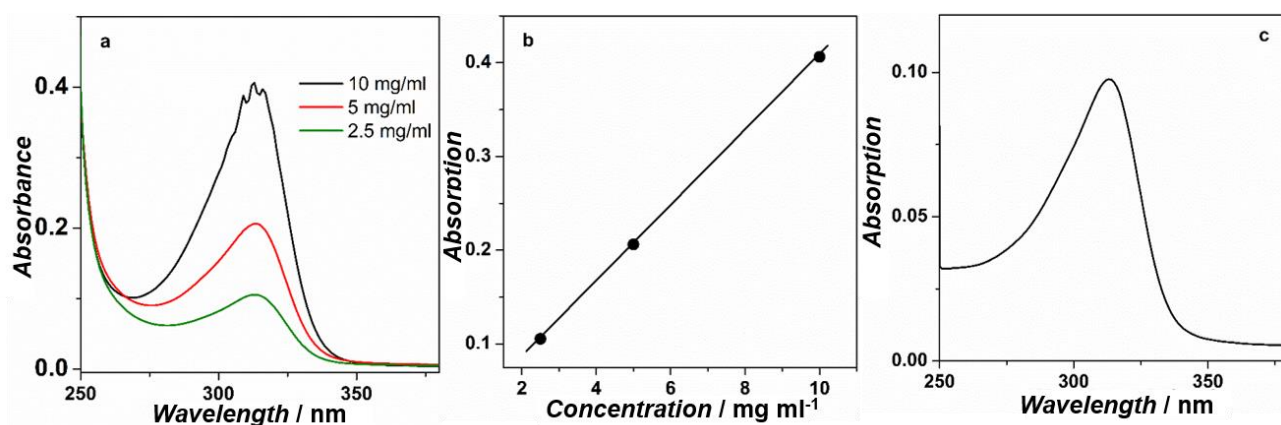


Figure S15 a) UV-Vis spectrum of 4-Methoxybenzenediazonium tetrafluoroborate solution at different concentrations. b) Plot of absorption at 315 nm versus concentration. c) UV-Vis spectrum of 4-Methoxybenzenediazonium tetrafluoroborate solution after molecular modification of NiO nanoparticles. The concentration of diazonium salt remaining in solution is estimated to be 2.43 mg/ml and the loaded molecule amount is estimated to be 2.37 nm⁻².

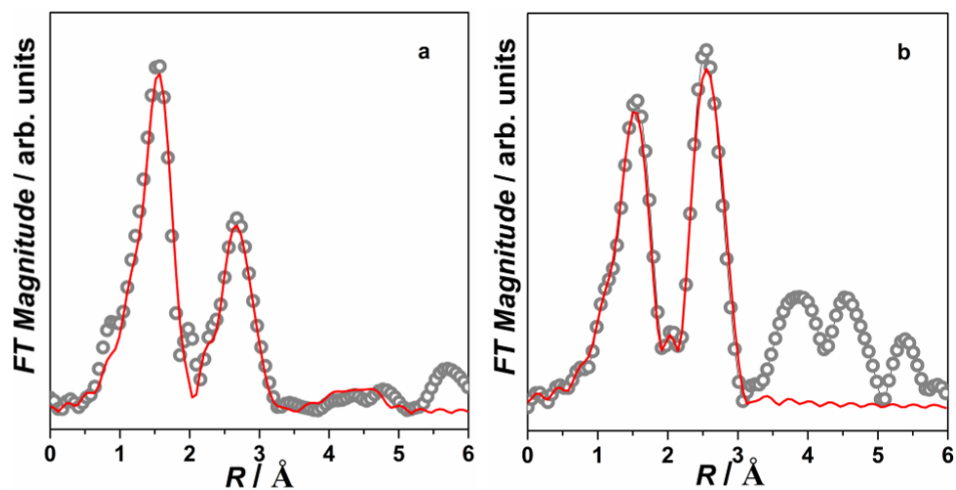


Figure S16 Fitting of the Fourier transformed k^3 -weighted EXAFS spectra of a) NiO and b) NiO- C_6F_5 samples.

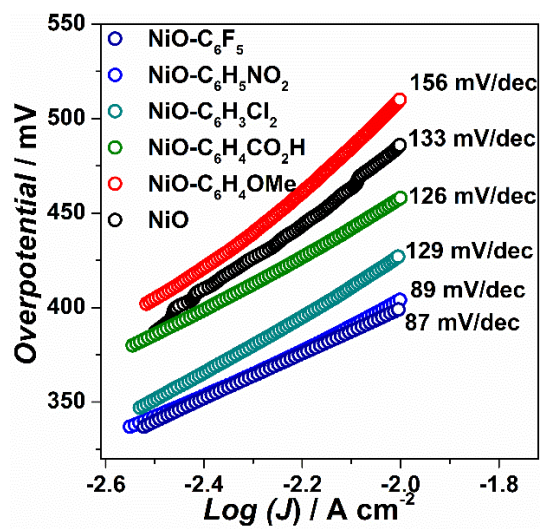


Figure S17 Tafel slopes of bare NiO and all modified NiO samples on glassy carbon electrode.

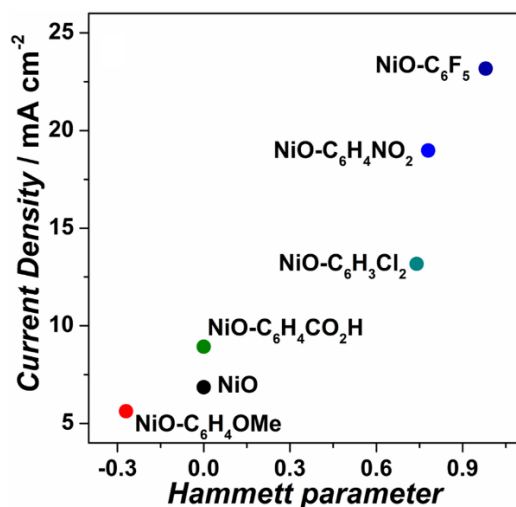


Figure S18 Current densities measured at 450 mV overpotential of bare NiO and all modified NiO samples.

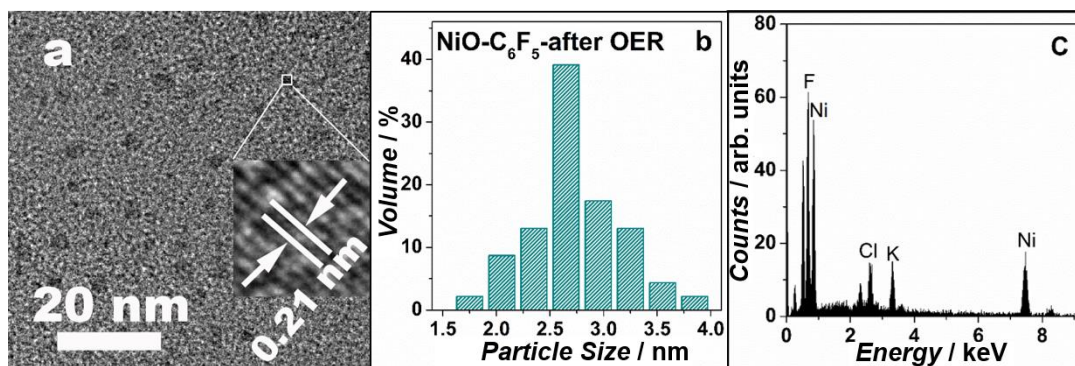


Figure S19 a) TEM pattern, b) Particle size distribution and c) EDS spectrum of NiO-C₆F₅ sample after OER electrolysis under 320 mV overpotential for 10 h.

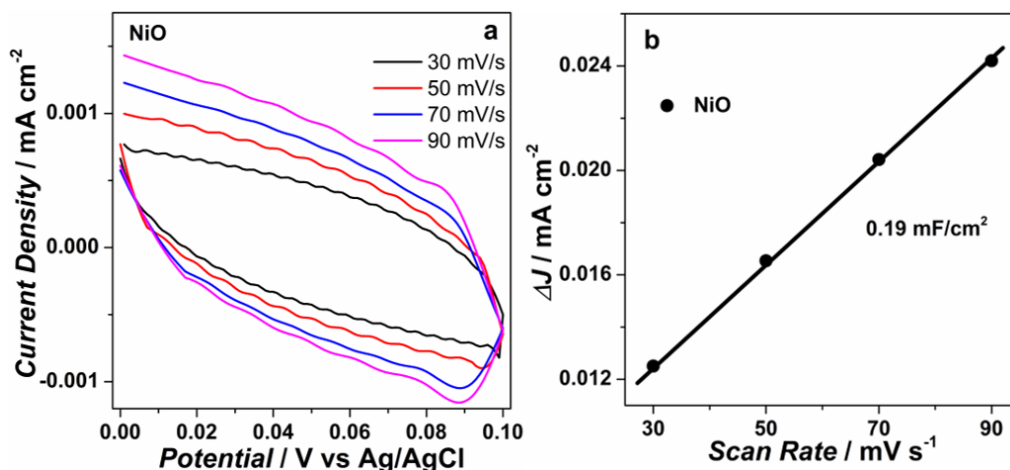


Figure S20 a) Cyclic voltammety curves of NiO at different scan rates. b) ΔJ ($=J_a - J_c$) of NiO plotted against the scan rates.

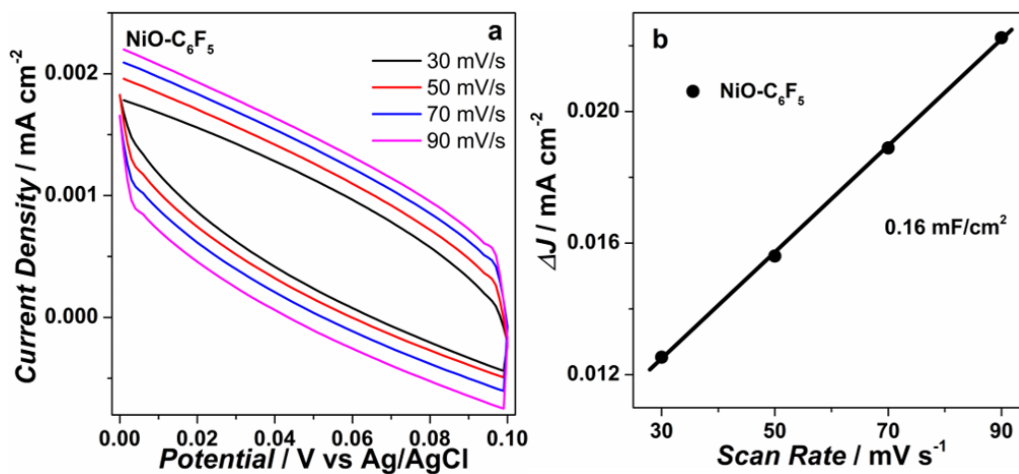


Figure S21 a) Cyclic voltammograms of NiO-C₆F₅ at different scan rates. b) ΔJ ($=J_a - J_c$) of NiO-C₆F₅ plotted against the scan rates.

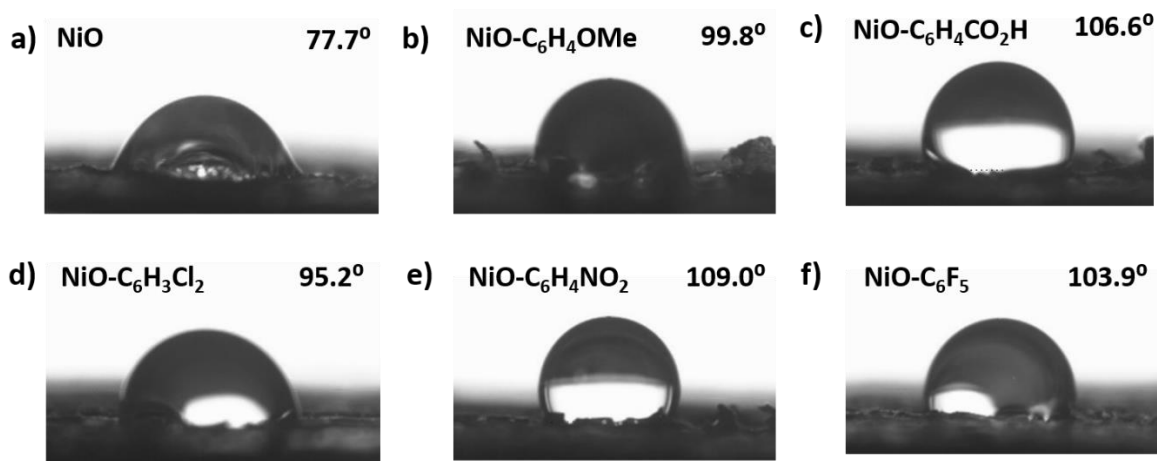


Figure S22 Water contact angles of bare NiO and all molecular modified NiO samples.

Table S1 Structural parameters of NiO and NiO-C₆F₅ extracted from EXAFS refinement. The standard deviations in parentheses were obtained from k³-weighted least square refinement of the EXAFS function $\chi(k)$ and do not include systematic errors of the measurement.

Sample	Path	R (Å)	CN	ΔE (eV)	σ^2 (Å ²)
NiO-d	Ni-O	2.023(1)	5.97	-13.108(3)	0.0057(1)
	Ni---Ni	3.101(2)	6.91		0.0097(1)
NiO-C ₆ F ₅	Ni-O	2.043(2)	5.98	-9.895(4)	0.0069(2)
	Ni---Ni	2.974(2)	7.96		0.0094(1)
	Ni---C	2.728(2)	0.48		0.0087(1)